

## A NUMERICAL GRID GENERATION SCHEME FOR THERMAL SIMULATIONS IN LAMINATED STRUCTURES

Patricia.H. James\*, Christopher S. Welch<sup>o</sup>,  
and William P. Winfree  
MS 231  
NASA, Langley Research Center  
Hampton, VA 23665

### INTRODUCTION

Significant efforts are being made to improve the safety of the solid rocket motor (SRM) for the shuttle. The SRM is a laminated structure consisting of four layers of materials: a steel casing, bonded to NBR insulation, the liner, and the propellant. One of the candidate inspection techniques is a thermal technique which analyzes the response of the SRM to an external heat source for detection of disbonds at the interfaces between the steel, NBR and fuel. Computational simulations of experimental measurements can provide limits of the effectiveness of the technique and easily assume a variety of different defect geometries to determine their detectability without the expense of making many different samples. Simulations can also provide useful information for the experimenter including the heating protocol that will provide the greatest contrast and the typical flaw size that can be detected.

The first step in a computational simulation is to discretize the field of interest. This is accomplished through a mapping from a uniform computational domain ( $\xi, \eta$  coordinates) to a nonuniform, boundary conforming physical domain ( $x, y$  coordinates) that represents the physical geometry. A proper mapping is fundamental to an accurate computational simulation; the discrete representation of the physical geometry should reflect a knowledge of the physics of the experiment coupled with an understanding of the mathematics of the simulation. This discrete representation of the physical geometry should accurately define the boundaries of the field of interest. The grid must also be refined enough to properly solve the governing equations in regions of large gradients while minimizing the total number of grid points in order to diminish the CPU time required to solve the model. Once a properly constructed grid has been defined with associated boundary and initial conditions, an accurate numerical solution to the partial differential equation (PDE) at these discrete locations can be obtained.

For numerical simulations to be credible, the erroneous results that can be incurred simply through an unacceptable mapping must be understood and corrected. Only then can a finite representation of the differential equations be correctly solved. For example, the

---

\*Analytical Services & Materials

<sup>o</sup>College of William & Mary

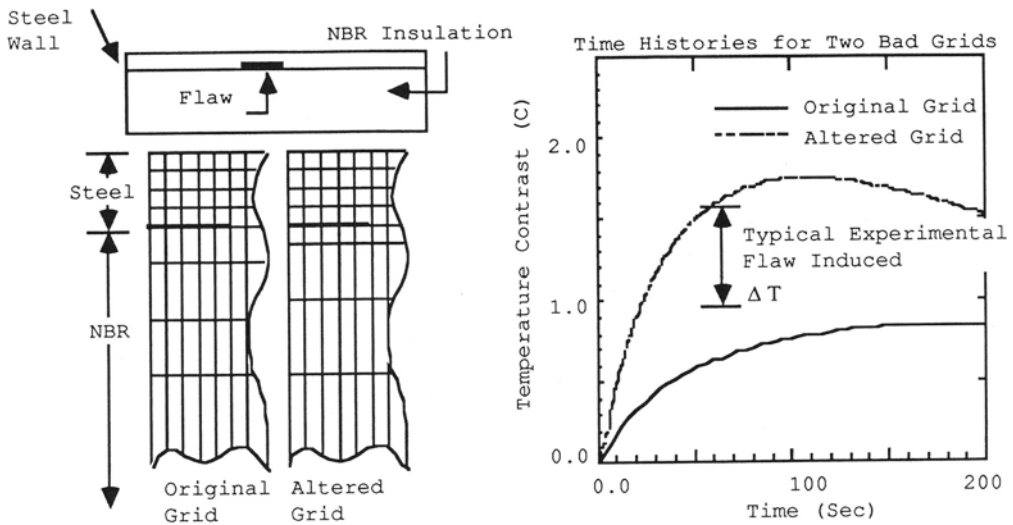


Fig. 1. Simple grid structure inadequate for thermal analyses

seemingly reasonable grid shown below (Fig. 1.) was used to model a thermally loaded "SRM" sample. The sample was modeled as a two-layered laminate with a 1.2 cm thick layer of steel having a thermal conductivity of  $36 \text{ W/(m}^\circ\text{C)}$ , a density of  $7750 \text{ Kg/cubic m}$ , and a heat capacity of  $460 \text{ J/(Kg}^\circ\text{C)}$ , bonded to a 8.8 cm thick layer of NBR insulation having a thermal conductivity of  $0.242 \text{ W/(m}^\circ\text{C)}$ , a density of  $1208 \text{ Kg/cubic m}$ , and a heat capacity of  $1923 \text{ J/(Kg}^\circ\text{C)}$ . The flaw width was 1/18th the width of the entire sample. The simulation convected heat into the steel face for 200 seconds ( $h = 7.28 \text{ W/(m}^\circ\text{C)}$ ). The grid consisted of  $12 \times 37$  grid points, taking advantage of the symmetry along the x-axis by reflecting the solution and therefore halving the number of grid points needed. By slightly altering the location of only two grid lines in the insulation, the temperature contrast time histories (defined as the difference between the temperature of a node directly over the flaw and the temperature of a node at the far edge of the sample as a function of time) for nodes on the front face changed dramatically. This discrepancy is larger than the experimentally measured temperature contrast over a delamination 1/12th the width of the SRM samples when heated for 1 minute with  $55^\circ\text{C}$  water (approximately  $0.5^\circ\text{C}$ ).

Much research has been done in the development of numerical grid generation schemes for computational fluid dynamics [1], [2], [3]. Many of the principles developed in this field can be applied to numerically modeling NDE problems. The necessity of a "good" mapping between the physical and computational domains is very pronounced in the case of laminated structures, in which large material property discontinuities exist between layers. For solutions to the heat equation as a thermal load is applied to the model, clustering of grid points at the material interface is required in order to resolve the details of the heat flux in this region.

#### GENERAL MESH GENERATION TECHNIQUES

The object of a grid generation algorithm is to transform a uniform mesh in the computational domain to a nonuniform, boundary-conforming grid in the physical domain. Research has shown that the mapping from the computational space into the physical space must be one-to-one and no grid lines should cross [4]. Additionally, the grid

points need to be clustered in regions of large gradients. Mesh generation codes should implement equations that avoid skewness and large cell aspect ratios if feasible; large cell aspect ratios degrade the convergence rate to steady state. Finally, it is very important to retain a smooth variation of the distance between grid lines in order to provide continuous transformation derivatives (metrics) between the physical domain and the computational domain [5].

There are many different methods of grid generation, and each method is useful for specific cases. For simple boundary shapes, such as typical test samples, algebraic generation methods are usually the most efficient. Therefore, an algebraic grid transformation method was chosen for modeling the laminated geometries, and its implementation is explained in the next section. It has been shown that when the variation in spacing in the interior of the model should be large, the interpolating functions best suited for algebraic grid generation methods are the hyperbolic tangent and the hyperbolic sine [6]. For this application, an equation involving the hyperbolic sine was used.

#### THE TRANSFORMATION EQUATION

Typically, large spatial temperature gradients will occur at the material boundaries of the SRM, and small grid spacing is required in these regions as compared to the spacing necessary in the insulating layer. The laminated structure of the SRM, and the rectangular geometry of the samples, simplifies the mapping conceptually and computationally. A transformation equation capable of refining the mesh about some interior point  $x_c$  is shown below.  $\tau$  is the "stretching" parameter that varies from zero (to produce a uniform grid) to large values (which yield the most refinement near  $x=x_c$ ),  $\xi$  is the coordinate in the computational domain that varies from zero to one in divisions equal to the total number of grid elements, and  $x$  is the location of the grid points in the physical domain which varies from zero to  $L$ , the length of the sample. This transformation has been shown to yield good results for fluid applications [7].

$$x = x_c \left\{ 1 + \frac{\sinh[\tau(\xi - B)]}{\sinh(\tau B)} \right\} \quad \text{Where} \quad B = \frac{1}{2\tau} \ln \left[ \frac{1 + (e^{-\tau} - 1)^{(\alpha/L)}}{1 + (e^{-\tau} - 1)^{(\alpha/L)}} \right] \quad (1)$$

#### COMPARISON TO ANALYTIC SOLUTION

To evaluate the effectiveness of the transformation equation and to illustrate the importance of a properly constructed grid, a case with a known analytic solution was modeled [8]. The physical model is shown below (Fig. 2.). Two bodies with different thermal properties and initial temperatures are brought into contact at some initial time  $t=0$ , with the simplifying assumption of zero contact resistance between the two layers. The structure is laminated as is the SRM, but it does not include the fundamental problem of the flaw between the laminae, nor the multiple layers of the SRM design. The material properties of the SRM samples (steel and NBR insulation) were used for the two layers. Initial conditions were set to 50°C in the steel and 0°C in the NBR, and the front face of the model was observed as it cooled. To properly resolve the temperature gradient at the interface, the grid points surrounding this region must be closely spaced. Very little change in temperature, however, will occur near the rear of the NBR. To minimize computation time while still maintaining sufficient accuracy, a grid with largely varying spacing is preferable having small spacing near the material boundary which gradually becomes larger in the insulation.

Simulations with different magnitudes of clustering the same number of grid points illustrate the importance of a sufficiently refined grid. For a uniform grid with 31 grid points distributed in a total width of 10 cm, the maximum error on the front face of the model was just over 3°C at 106 seconds. As the clustering parameter was increased to 11 for the same number of grid points, the maximum error was reduced to only 0.12°C at 7 seconds. In both cases the cluster location was at the material interface. The exact solution is compared to solutions using these two magnitudes of clustering in Fig. 2.

In terms of maximum percent error, the effect of increasing the clustering for this model is shown in Fig. 3. The method is shown to exhibit a predictable behavior when changing the clustering parameter; as  $\tau$  is increased at the material interface, the simulation more exactly represents the correct solution until a minimum in error is reached, whereupon further increasing  $\tau$  only increases the magnitude of the total error due to the increase in roundoff error. As expected, the CPU time is increased as a more exact solution to the governing equation is found. The effect of increasing  $\tau$  on CPU time is also shown in Fig. 3. However, the 24:1 reduction in error more than compensates for the 1:3.5 increase in CPU time.

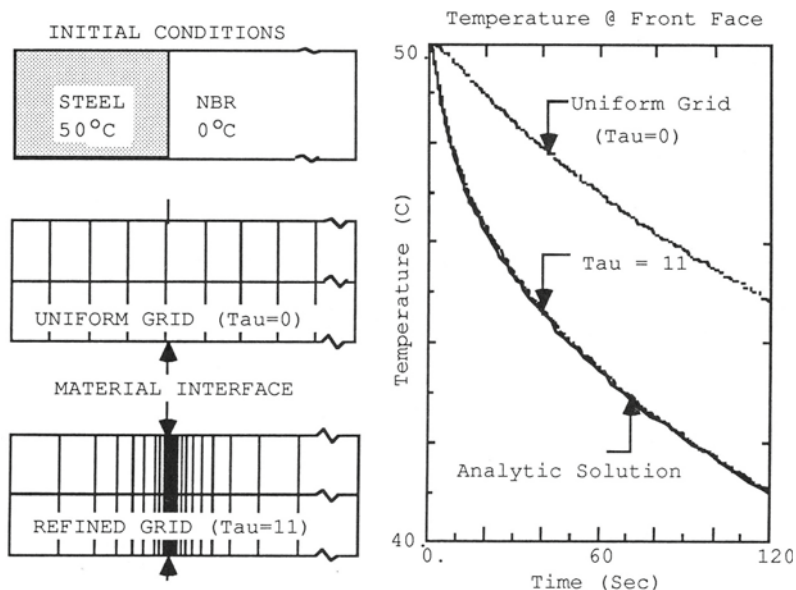


Fig. 2. A properly generated grid exhibits predictive behavior

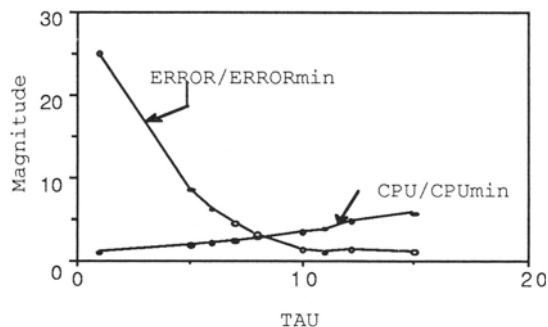


Fig. 3. Large reduction in error ratio / Small increase in CPU Ratio

# EFFECTS OF A PROPERLY GENERATED GRID ON THERMAL SIMULATIONS

The specific amount of clustering needed depends largely on the boundary and initial conditions and the material properties of the laminate. For the problem referred to in the introduction, where minor changes in the grid structure produced unacceptably large changes in the solution to the heat equation, a grid was generated using equation (1) with a clustering parameter of  $\tau=7$  (Fig. 4). Perhaps the most important requirement for generating a "good" grid is that of a smooth derivative in the distance between grid lines. The derivative of the spacing between grid lines for the original grids are compared below with the grid produced from the transformation equation in Fig. 5. Note the smoothness in the derivative for the grid generated using the transformation equation, while the spatial derivatives for the original and slightly altered grids are not smooth.

The related relative temperature time histories are also shown below (Fig. 6.). Note that the slightly altered grid produces a temperature history relatively close to the "Good" grid solution. This phenomena is probably due to the minimum in spacing at the material interface for the altered grid, which does not occur in the case for the original grid (as shown in Fig. 5.).

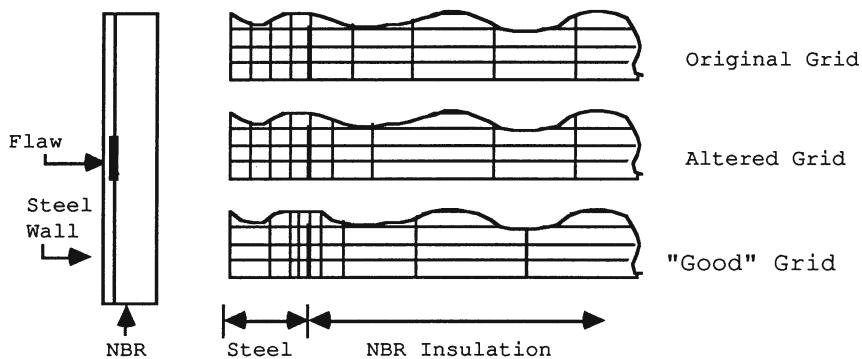


Fig. 4. Comparison of grid structures

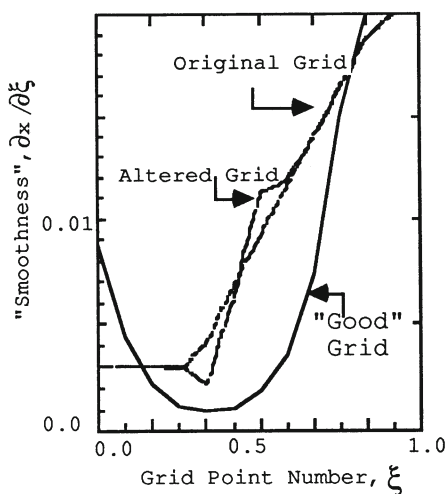


Fig. 5. Transformation equation yields smooth spatial derivative

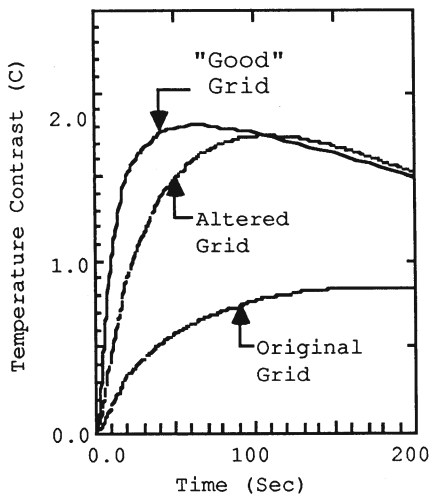


Fig. 6. Comparison of time histories for three grids

## ERROR ANALYSIS

Large changes in spacing across the grid can introduce significant truncation error. Thompson, et al.[9] showed that as grid points are added, the truncation error is reduced by the square of the number of additional grid points for the same transformation equation. The truncation error Thompson derived is

$$T.E. = -\frac{1}{2} x_{\xi}^2 f_{\xi\xi} - \frac{1}{6} x_{\xi}^3 f_{\xi\xi\xi} \quad (2)$$

Where  $x$ , the spatial coordinate in the physical domain, is a function of  $\xi$  ( $0 \leq \xi \leq 1$ ), the coordinate in the computational domain. The general transformation function,  $f$ , is also a function of  $\xi$ . The last term of the series occurs even for uniform spacing, and the first term is dependent on the rate of change of spacing. For a particular transformation function, doubling the spacing from one grid point to the next can introduce large truncation errors. To examine the errors associated with the spatial derivatives of the grids for thermal NDE applications, consider the discrete form of the heat equation

$$\frac{1}{\alpha} \frac{\partial T}{\partial \tau} = \frac{\left( \frac{\partial T}{\partial x} \right)_{j+1/2} - \left( \frac{\partial T}{\partial x} \right)_{j-1/2}}{x_{j+1/2} - x_{j-1/2}} \quad (3)$$

If the spacing from an arbitrary element,  $j$ , to the two successive elements changes in the following manner (see Fig. 7.)

$$(\Delta x)_{j+1} = \beta (\Delta x)_j \quad \text{AND} \quad (\Delta x)_{j+2} = \gamma (\Delta x)_j \quad (4)$$

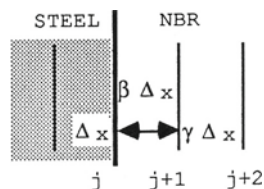
then it is easily shown that the relative error incurred through large changes in spacing is

$$\text{ERROR} \propto C_1 \Delta T_{j+1} + C_2 \Delta T_{j+2} + C_3 \Delta T_j \quad (5)$$

$$\text{Where } C_1 = 2 \left( 1 - \frac{1}{\beta(\beta+1)} - \frac{1}{\beta(\beta+\gamma)} \right), \quad C_2 = \frac{2}{\gamma(\gamma+\beta)} - 1 \quad \text{And} \quad C_3 = \frac{2}{\beta+1} - 1$$

(Note that if  $\beta = \gamma = 1$ , then  $\text{ERROR} = 0$ ) Consider the elements surrounding the material interface. The error will be dominated by the  $C_1$  term, since the temperature gradient is largest across the interface. The error parameters for the grids illustrated in Fig. 4. are tabulated below for the elements just before and after the material boundary. Comparison of the critical parameter,  $C_1$ , illustrates the magnitude of the effect of changes in grid spacing; the relative error due to nonuniform spacing at one spatial location is approximately 52 times greater in the original grid than in the computationally generated "Good" grid!





Type of Grid		C1	C2	C3
Original Grid	( $\beta=1.38$ ; $\gamma=2.62$ )	1.04	-0.81	-0.16
Altered Grid	( $\beta=0.83$ ; $\gamma=3.33$ )	0.10	-0.86	0.09
"Good" Grid	( $\beta=0.95$ ; $\gamma=1.39$ )	0.02	-0.39	0.03

Fig 7. Relative error comparison

#### COMPARISON TO EXPERIMENTAL DATA

Having developed a properly generated grid, the method can now be applied to real problems involving flaws between laminates such as those that would exist for the SRM samples. How the simulation compares to experimental data depends on many different factors. A simple physical model (Fig. 8.) was chosen to compare the simulation with the experiment in order to reduce the factors that could possibly introduce discrepancies. A key feature of the geometry includes the laminated structure of the SRM, where the first layer is a conductor (steel), and the second layer is an insulator (plexiglas). To simulate a flaw, a half inch wide section of the plexiglas was excised from the back of the sample.

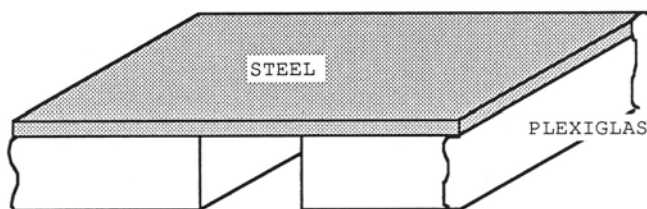


Fig. 8. Geometry of experimental sample

The sample was heated from the steel side for 15 seconds with a heat gun, and temperature data on the steel face was collected by an infrared camera as the sample cooled. Two of these profiles are shown below. The high amplitude curve was the first data set taken after heating, and the lower curve was acquired 40 seconds later.

The application of a thermal load by the heat gun was modeled as a flux input boundary condition and applied for 15 seconds, then removed to observe the model as it cooled. Two temperature profiles across the front face for the corresponding times are shown below.

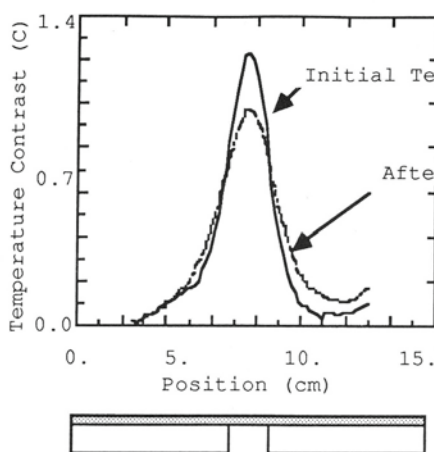


Fig. 9. Experimental data

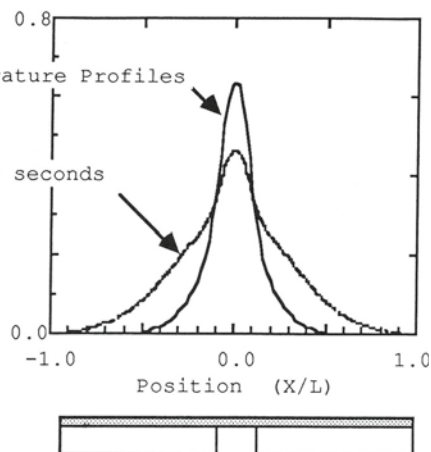


Fig. 10. Computational data

The comparison of the experimental data with the computational results is reasonable. The simulation clearly delineates the presence of a disbond between the laminatae. Since the passage of heat to the second material is inhibited directly over the flaw, the disbond is observed as a temperature increase at the front face of the sample. The grid was highly clustered around the region of the largest temperature gradient as was discussed previously. The change in amplitude during the 40 seconds between data sets for the experimental case is approximately  $0.3^{\circ}\text{C}$ , and approximately  $0.2^{\circ}\text{C}$  for the simulation. The fact that the exact magnitudes of the two figures differ slightly can be attributed to many different facts, not least of which is the uncertainty of the exact magnitude of the flux input from the heat gun. An additional discrepancy between the data sets is that the experimental data does not spread out as much as the computational data. This is probably due to uneven heating of the sample during the experiment.

## CONCLUSIONS

A method for numerically generating a grid for laminated structures with simple geometries has been presented. The rationale for using such a method has been discussed, including the importance of the requirement for a grid generation technique which gives a smooth distribution of grid points across the solution domain. The error involved for a nonuniform grid with an irregular distribution is shown to be prohibitive.

Comparing the method for a model where an exact solution is known has provided a measure of absolute error encountered by altering the distribution of a fixed number of grid points. For laminated materials where the material properties vary greatly between layers, significant error has been shown to exist for grids where the temperature gradients have not been properly resolved. Furthermore, comparisons of experimental and numerical results show reasonable agreement and predictive power of the computational method.



## REFERENCES

1. Joe F. Thompson, Z.U.A. Warsi, and C.W. Mastin, "Boundary-Fitted Coordinate Systems for Numerical Solutions of Partial Differential Equations - A Review:", Journal of Computational Physics, 47,1, (1982).
2. Peter R. Eiseman, and Robert Smith, "Mesh Generation Using Algebraic Techniques", Ed. Robert E. Smith, NASA CP-2166, (1980).
3. R.L. Sorenson, "A Computer Program to Generate Two-Dimensional Grids About Airfoils and Other Shapes by the Use of Poisson's Equations", NASA Ames Research Center, NASA TM 81198, (1980).
4. Dale A. Anderson, John C. Tannehill, and Richard H. Pletcher, Computational Fluid Mechanics and Heat Transfer, (Hemisphere Publishing Corporation, McGraw-Hill Book Company, New York, 1984), p. 521.
5. Anderson, Tannehill, and Pletcher, p. 521.
6. Joe F. Thompson, Z.U.A. Warsi, and C.W. Mastin, Numerical Grid Generation - Foundations and Applications, (North-Holland Press, New York, 1985), p.306.
7. Anderson, Tannehill, and Pletcher, pp.250-251
8. H.S. Carslaw and J.C. Jaeger, Conduction of Heat in Solids, (Oxford University Press, London, 1959), pp. 319-324.
9. Thompson, Warsi, and Mastin, Numerical Grid Generation Foundations and Applications, (North-Holland Press, New York, 1985), pp. 171-184.